Acta Pharmaceutica Sinica B 2024;14(5):2137–2152

Chinese Pharmaceutical Association
Institute of Materia Medica, Chinese Academy of Medical Sciences

Acta Pharmaceutica Sinica B

www.elsevier.com/locate/apsb
www.sciencedirect.com

ORIGINAL ARTICLE

Small molecule conjugates with selective estrogen receptor β agonism promote anti-aging benefits in metabolism and skin recovery

Tarik Zahr[a,b,†], Vijay K. Boda[c,d,†], Jian Ge[e,f,†], Lexiang Yu[a,g], Zhongzhi Wu[c,d], Jianwen Que[e,f,h,*], Wei Li[c,d,*], Li Qiang[a,g,*]

[a]*Naomi Berrie Diabetes Center, Columbia University, New York, NY 10032, USA*
[b]*Department of Molecular Pharmacology and Therapeutics, Columbia University, New York, NY 10032, USA*
[c]*Department of Pharmaceutical Sciences, College of Pharmacy, University of Tennessee Health Science Center, Memphis, TN 38163, USA*
[d]*Drug Discovery Center, College of Pharmacy, University of Tennessee Health Science Center, Memphis, TN 38163, USA*
[e]*Division of Digestive and Liver Diseases, Columbia University, New York, NY 10032, USA*
[f]*Center for Human Development, Columbia University, New York, NY 10027, USA*
[g]*Department of Pathology and Cell Biology, Columbia University, New York, NY 10032, USA*
[h]*Department of Medicine, Columbia University, New York, NY 10032, USA*

Received 22 October 2023; received in revised form 13 December 2023; accepted 5 January 2024

KEY WORDS

Estrogen receptor β;
Aging;
Metabolism;
Skin injury;
Muscle metabolism;
Small molecule conjugates;
Regeneration;
Adiposity

Abstract Estrogen is imperative to mammalian reproductivity, metabolism, and aging. However, the hormone activating estrogen receptor (ERs) α can cause major safety concerns due to the enrichment of ERα in female tissues and certain malignancies. In contrast, ERβ is more broadly expressed in metabolic tissues and the skin. Thus, it is desirable to generate selective ERβ agonist conjugates for maximizing the therapeutic effects of ERs while minimizing the risks of ERα activation. Here, we report the design and production of small molecule conjugates containing selective non-steroid ERβ agonists Gtx878 or genistein. Treatment of aged mice with our synthesized conjugates improved aging-associated declines in insulin sensitivity, visceral adipose integrity, skeletal muscle function, and skin health, with validation *in vitro*. We further uncovered the benefits of ERβ conjugates in the skin using two inducible skin injury mouse models, showing increased skin basal cell proliferation, epidermal thickness, and wound healing. Therefore, our

*Corresponding authors.
E-mail addresses: jq2240@cumc.columbia.edu (Jianwen Que), wli@uthsc.edu (Wei Li), lq2123@cumc.columbia.edu (Li Qiang).
[†]These authors made equal contributions to this work.
Peer review under the responsibility of Chinese Pharmaceutical Association and Institute of Materia Medica, Chinese Academy of Medical Sciences.

https://doi.org/10.1016/j.apsb.2024.01.014

ERβ-selective agonist conjugates offer novel therapeutic potential to improve aging-associated conditions and aid in rejuvenating skin health.

1. Introduction

Estrogen is integral to mammalian physiology. In addition to its traditional implications in reproductive biology, emerging data reveals an expansive role for this hormone in health and disease[1]. Estrogen is important for the regulation of glucose and lipid metabolism, and an imbalance in estrogen levels leads to metabolic dysfunction[2]. Examples include a predisposition to visceral obesity, metabolic syndrome, and type 2 diabetes[3,4]. Low estrogen levels correlate with increased body weight, hyperglycemia, glucose intolerance, and an impaired sensitivity to insulin[5]. Estrogen also modulates the differentiation of adipocytes and their ability to store lipids[6], which consequently alters the response to insulin. The decline in estrogen in women experiencing menopause increases the risk of metabolic changes in adipocytes as well as changes in energy balance and glucose homeostasis[7–9]. Moreover, the influence of estrogen on the postmenopausal aging process can be applied to muscle and skin health. In the muscle, estrogen promotes mitochondrial function and thus exercise endurance, whereas a decrease in the hormone is associated with muscle frailty[10]. In the skin, estrogen aids in preserving collagen, maintaining moisture, and preventing thinning, atrophy, drying, wrinkling, and delayed wound healing in response to injury[11,12].

Estrogens function through activating estrogen receptors (ERs), which include three subtypes, ERα, ERβ, and G protein-coupled estrogen receptor (GPER). These receptors vary in structure, distribution, and function. ERα and ERβ are the two main forms with comparable binding affinity for estrogens[13] but different in tissue expression and implications in metabolism and diseases[14]. ERα is highly expressed in female reproductive tissues, and its activation increases the risk for cancers in the breast, prostate, and uterus[15]. In contrast, ERβ is broadly expressed in reproductive tissues of both sexes as well as in other tissues[16]. Interestingly, the roles for ERα and ERβ in the tumor microenvironment have not been fully characterized, with some sources indicating a tumor suppressive role for ERβ as opposed to ERα[17,18]. For example, the loss of ERβ expression is common in colorectal cancer, in line with enhanced survival in breast cancer with higher ERβ expression[19,20]. Activation of ERβ inhibits cell proliferation in early prostate cancer and benign prostatic hyperplasia[21]. Frustratingly, estrogens do not have satisfactory distinguishment between ERα and ERβ[22]. As such, ERs have become popular yet controversial targets for therapeutic purposes.

Previous reports allude to the important roles of ERβ in metabolically active tissues including adipose tissue and skeletal muscle[14]. Genetic evidence demonstrates the association of activating ERβ with metabolic benefits. For example, a polymorphism study revealed that one haplotype in the gene encoding ERβ, *ESR2*, presents a positive correlation with reduced obesity risk in postmenopausal women[23]. More recently, decreased levels of *ESR2* mRNA in visceral adipose tissue and subcutaneous white adipose tissue (sWAT) have been shown to increase the risk for obesity in humans. The study also showed that weight loss restores the transcriptional activity of *ESR2*[24]. Hence, the use of selective ERβ agonists may hold value in promoting metabolic improvements while preventing the undesirable outcomes stemming from ERα activation[16]. In line with this, activation of ERβ in diet-induced obese mice shows a multitude of benefits, promoting adipocyte browning, improving mitochondrial function and energy expenditure, lowering body weight and fat mass, enhancing insulin sensitivity and glucose tolerance, and reducing hepatic lipid accumulation[25–27]. Furthermore, estradiol-derived selective ERβ agonists significantly inhibit lipogenesis in adipose tissue of obese female Wistar rats through the downregulation of SRE binding protein 1 (SREBP-1), fatty acid synthase (FASN), and lipoprotein lipase (LPL)[28]. ERβ activation also stimulates skeletal muscle growth and regeneration in male rats and female mice[29,30]. Further studies revealed the effects are mediated by inducing anabolic activity in muscle, contributing to increased fiber size and the availability of serum growth factors in the presence of selective ligands for ERβ, but not ERα[31]. Therefore, a derivation of selective ERβ agonists is critical for leveraging the therapeutic potential of ERs while circumventing their safety concerns.

Beyond metabolic regulation, a decline in ERβ levels has been linked with aging in both sexes[32–34]. Aging impacts many organs, including the skin[35]. Interestingly, the use of selective ERβ agonists can curb UV-induced photodamage and skin wrinkling in a mouse model of photoaging[36]. Thus, selective ERβ agonists seem to have additional anti-aging benefits. In this study, we developed and explored the function of selective ERβ agonist conjugates and their derivatives as anti-aging agents. Genistein is a naturally occurring compound, and GTx878 is a synthetic analog of genistein. Both compounds are potent ERβ agonists, but their relatively high polarity leads to limited absorption efficiency upon topical application[37–39]. To modify the physical and chemical properties of these compounds, we proposed designing small molecule conjugates using ester links to generate a unique class of ERβ agonists. Ester molecules are rapidly hydrolyzed by esterase upon absorption, offering an efficient route for compound delivery without the risk of chemical toxicity[40]. These selective ERβ agonist conjugates displayed potent effects in alleviating insulin resistance, adipose degeneration, and muscle frailty in aged mice. Additionally, the application of the agonist conjugates promoted skin healing after injury. Our study thus proposes extensive anti-aging benefits using selective ERβ agonist conjugates.

2. Materials and methods

2.1. Animal studies

Mice were bred and housed at 22 ± 1 °C under a 12-h light/12-h dark cycle, with access to food and water *ad libitum*. All mice

were on a C57BL/6J background and fed on a standard diet (Purina). 24-Month-old aged mice began treatment with a synthesized ERb selective agonist (VB-165) for 6 weeks. The compound was intraperitoneally injected at a dose of 20 mg/kg.bw (body weight) in the vehicle solution (10% DMSO, 5% Tween-20) for 5 days a week, followed by body composition monitoring using EchoMRI. The serum triglyceride profile was obtained using Infinity Triglycerides Liquid Stable Reagent (Thermo Fisher Scientific). Serum blood cell counts were conducted at room temperature using a standard analyzer (GENESIS, Oxford Science). For insulin tolerance tests (ITT), mice were fasted for 4 h (10:00 AM−2:00 PM) and given intraperitoneal injections of 0.75 U/kg.bw human insulin. Blood glucose levels were assessed *via* tail vein bleeding using a OneTouch glucometer at pre-injection (0 min) followed by post-injection time points (15, 30, 45, and 60 min). Animal protocols were reviewed and approved by the Columbia University Animal Care and Utilizations Committee and are performed in accordance with NIH guidelines.

2.2. The excision-induced skin injury model

Mice were anesthetized with an intraperitoneal injection of tribromoethanol (350 mg/kg). After shaving the dorsal hair, the skin was sterilized with a swab soaked in 70% ethanol, and a sterile punch biopsy tool (6 mm, SHARD® Premium A750-BP60) was used to generate dorsal skin wounds. Mice were monitored every 10 min on a warm pad until they woke up from anesthesia. Oculentum, an ointment, was applied to the eyes before and after injury induction. Compounds (1 mmol/L ERβ agonist or vehicle) were applied to the injured area on the skin every other day for one month.

2.3. The frostbite-induced skin injury model

Oculentum was applied to the eyes before and after injury. Dorsal hair was shaved 24 h before induction of injury. On Day 0, magnets with a 0.5-inch diameter were cooled down on dry ice for 15 min. Mice were anesthetized, and the skin area was sterilized using the same method mentioned above. The center of the experimental skin area was lifted and exposed to two frozen magnets for 1 min and subsequently replaced with two new frozen magnets after every 1-min interval to ensure temperature consistency. This freezing procedure was continued for a total of 5 min. Upon completion, magnets were removed, and the skin was left to thaw completely. Mice were monitored every 10 min on a warm pad during recovery from anesthesia. Compounds (1 mmol/L ERβ agonist or vehicle) were applied to the injured skin area every other day for one month.

2.4. Cell culture

HEK-293 and C2C12 cells were cultured in DMEM (Dulbecco's modified Eagle's medium) with 4.5 g/L glucose, supplemented with 10% fetal bovine serum (FBS) and appropriate antibiotics. HEK-293 cells were plated in 48-well plates 24 h prior to transfection. DNA was delivered to cells using TransIT®-293 transfection reagent and Opti-MEMi reduced serum medium. Plasmids used for reporter activity assay were 3x-ERE-TATA-Luc (Addgene #11354), pCMV-hERa (Addgene #101141), and pcDNA-Flag-hERb (Addgene #35562). Luciferase activity was assessed using a Dual-Luciferase Reporter Assay System (Promega, E1980) and measured with a plate reader (Tecan Infinite F200). C2C12 cells were plated in 12-well plates and differentiated to myotubes in media containing 2% horse serum for 7 days[41,42]. Agonists used *in vitro* were administered on Days 1, 3, and 5 of differentiation at 1 mol/L concentration. Plasmids used for shRNA studies in C2C12 cells were pLL3.7 Scr shRNA (Addgene #59299) for sham and pLV-shEsr2 (Addgene #120722) for ERβ knockdown. For virus packaging, psPAX2 (Addgene #12260) and pMD2.G (Addgene #12259) were used. Transfection of plasmids was done in myoblasts before differentiation. 3T3-L1 preadipocytes (ATCC) were cultured in DMEM, 10% fetal calf serum (FCS), and 1% penicillin−streptomycin. Two days after reaching confluence, adipogenesis was induced with a cocktail containing 0.5 mmol/L 3-isobutyl-1-methylxanthine (IBMX), 1 μmol/L dexamethasone, and 10 μg/mL insulin for 2 days and replaced with full medium containing 10 μg/mL insulin[43]. 1 mmol/L agonist conjugates were kept in the medium during differentiation. Differentiated adipocytes were stained for neutral lipids using Oil Red O and BODIPY, as described previously[43,44]. Skin basal cells were isolated from neonatal mice. Upon euthanasia, limbs and tails were completely excised. The entire skin was then peeled off and washed with PBS, followed by incubation with 4 mg/mL dispase in basal medium (CC-3156, Lonza) and rotated overnight at 4 °C. The epidermis was separated and exposed to trypsin at room temperature for 20 min. As a result, basal cells were released and collected from the epidermal sheet. These isolated basal cells were cultured in their respective growth medium (CC-4162, Lonza) on an extracellular matrix-coated dish for further experiments.

2.5. Histology

Tissue samples were fixed in 10% formalin overnight, switched to 70% ethanol, and embedded in paraffin. Paraffin sections of 6 μm in thickness were obtained on charged slides. High-resolution brightfield images were taken at 20 × on an Olympus IX71 microscope equipped with a DP73 camera. Quantification of adipocyte size was conducted in Adiposoft, an automated software for the cellular analysis of adipose tissue available as a downloadable plug-in for Fiji.

2.6. Immunohistochemistry

Skin samples were sectioned (longitudinal) onto slides at 7 μm thickness, deparaffinized, and rehydrated in a series of ethanol washes of decreasing dilution. Slides were immersed in buffer (H-3300, Vector Labs) and pressure cooked for antigen retrieval. Slides were washed and blocked with 10% donkey serum for 45 min at room temperature. Primary antibodies anti-p63, 1:300 (Cell Signaling Technology, 13109S) and anti-Ki67, 1:200 (Invitrogen, 14-5698-82) were incubated overnight at 4 °C, washed, and followed with secondary antibody incubation. Slides were washed and mounted in media containing DAPI for imaging by confocal microscopy (Zeiss LSM 710 Confocal Microscope and Leica Stellaris 8 Confocal Microscope) at 20 × (0.75 NA) or 60 × (1.4 NA oil) objective lenses.

2.7. Quantitative real-time PCR

RNA was isolated using a Tri-Isolate RNA Pure Kit (IBI Scientific). A total of 1 μg RNA was used for cDNA synthesis with an Applied Biosystems High-Capacity cDNA Reverse Transcription Kit (Thermo Fisher Scientific). Gene expression was determined

using quantitative PCR, performed on a Bio-Rad CFX96 Touch Real-Time PCR Detection System using AzuraView GreenFast qPCR Blue Mix (Azura), and fold change was calculated using the ΔΔCt method, with Cyclophilin A (*CpA*) as the reference gene.

2.8. *Western blotting*

Tissues were homogenized using a Polytron homogenizer in the IntactProtein^{tm} Lysis Buffer (GenuIn Biotech, #415). The lysate was incubated on ice for complete lysis, followed by heat shock at 95 °C and centrifugation. SDS-PAGE and Western blotting were performed using standard procedures, and bands were detected using enhanced chemiluminescence (ThermoFisher Scientific, 32106). Antibodies used were anti-UCP1 (abcam, ab155117), anti-FABP4 (Cell Signaling Technology, #50699), anti-APN (ThermoFisher Scientific, PA1-054), anti-ADIPSIN (RnD Systems, AF5430), and anti-HSP90 (Proteintech, 13171-AP).

2.9. *Statistical analysis*

All values are presented as the mean ± standard error of mean (SEM), and statistical significance was determined using a student *t*-test from two groups. Two-way ANOVA was used to compare differences between groups with two independent variables. All data were analyzed in GraphPad Prism software version 9 (GraphPad Software, San Diego, CA, USA).

3. Results

3.1. *Synthesis of ERβ-selective agonist conjugates*

We first generated GTx878, a synthetic selective ERβ agonist, following a previously described method including 8 linear steps with an overall yield of 30% end products (Supporting Information Scheme S1). GTx878 has been demonstrated to curb a variety of conditions, such as angiogenesis and hypertension[45], obesity and adipose dysfunction[27], and malignancies in several tissues[46–48]. Next, we tested the conjugation of GTx878 with small chemicals. We first chose tranexamic acid (TXA), a synthetic derivative of lysine and an anti-fibrinolytic molecule. We reasoned that the conjugated product might have altered chemical characters and beneficial effects on improving skin conditions in aging since TXA significantly reduces melasma burden, a cosmetic problem predominantly observed among Asian demographics[49]. To commence the chemical synthesis of our compound, we used Boc-protected TXA to conjugate with GTx878. The Boc protecting group is known to benefit stability and permeability. Moreover, there are three sites containing free phenolic hydroxy groups available for esterification. The 8-OH group is involved in intramolecular hydrogen bonding as evidenced by a signal in the down-field region of its proton NMR spectra (Supporting Information Figs. S1 and S2). This is due to a chemical shift value around 13 ppm that requires harsh reaction conditions, like a strong base, to react. Among the other two OH functional groups, the one on the 4-hydroxyphenyl appears to be less reactive due to the presence of electron withdrawal.

Thus, 4-bromo-6,8-dihydroxy-2-(4-hydroxyphenyl)isoquinolin-1(2*H*)-one (GTx878) (0.30 g, 3.70 mmol) and (1*R*,4*R*)-4-(((*tert*-butoxycarbonyl)amino)methyl)cyclohexane-1-carboxylic acid (0.21 g, 3.70 mmol) were dissolved in anhydrous methylene chloride (50 mL) at room temperature under an argon. 4-Dimethylaminopyridine (0.21 g, 1.72 mmol) and 1-ethyl-3-(3-dimethylaminopropyl) carbodiimide hydrochloride (0.33 g, 1.72 mmol) were added at room temperature. The reaction mixture was stirred at room temperature overnight under argon atmosphere. The reaction was quenched by adding 50 mL of water at room temperature. The solution was extracted with ethyl acetate (3 × 50 mL). The extracts were dried over anhydrous $MgSO_4$, filtered, and concentrated under reduced pressure to dryness. The solid residue was purified by column chromatography (silica gel, CH_2Cl_2/acetone = 9/1 *v*/*v*) to give VB-165, 4-bromo-8-hydroxy-2-(4-hydroxyphenyl)-1-oxo-1,2-dihydroisoquinolin-6-yl (1*R*,4*R*)-4-(((*tert*-butoxycarbonyl)amino)methyl) cyclohexane-1-carboxylate, as a white solid (0.215 g, 42% yield). ^{1}H NMR (400 MHz, DMSO-d_6) δ 12.99 (s, 1H), 10.83 (s, 1H), 7.86 (s, 1H), 7.63−7.45 (m, 2H), 7.33−7.16 (m, 2H), 6.86 (s, 1H), 6.62 (d, J = 2.2 Hz, 1H), 6.38 (d, J = 2.2 Hz, 1H), 2.79 (t, J = 6.3 Hz, 2H), 2.59−2.51 (m, 1H), 2.15−2.02 (m, 2H), 1.82−1.69 (m, 2H), 1.43 (d, J = 3.4 Hz, 2H), 1.37 (s, 9H), 1.22 (s, 1H), 1.03−0.91 (m, 2H). ^{13}C NMR (100 MHz, DMSO-d_6) δ 174.77, 164.16, 156.66, 150.69, 138.32, 136.61, 133.69, 128.80, 128.45, 123.09, 104.71, 102.53, 78.49, 46.18, 42.75, 37.53, 29.37, 28.59, 28.43 (Supporting Information Figs. S3 and S4). HRMS (ESI): calculated for $C_{28}H_{30}BrN_2O_7$ is 585.1242 $[M-H]^-$; found 585.1253 (Supporting Information Fig. S5). Purity: 97.8% (Scheme 1A).

We also employed a natural steroid ERβ agonist, genistein, that has a distinct yet related chemical structure with therapeutic effects similar to GTx878. Genistein is a soy-derived isoflavone ERβ agonist and has received much attention from medicinal chemists and biologists due to its prophylaxis and anti-cancer properties[50]. We conjugated genistein with TXA in a similar fashion to yield a monoester derivative, JW-127, 5-hydroxy-3-(4-hydroxyphenyl)-4-oxo-4*H*-chromen-7-yl(1*R*,4*R*)-4-(((*tert*-butoxycarbonyl)amino)methyl)cyclohexane-1-carboxylate (Scheme 1B). ^{1}H NMR data of JW-127 revealed that the esterification occurred on 7-OH group. The 5 and 4^1-OH groups remained unreactive as evidenced by the presence of ^{1}H NMR signals at δ 12.96 and 9.65 ppm respectively (Supporting Information Fig. S5). ^{1}H NMR (400 MHz, DMSO-d_6) δ 12.96 (s, 1H), 9.65 (s, 1H), 8.51 (s, 1H), 7.39 (d, J = 8.4 Hz, 2H), 6.97 (d, J = 2.4 Hz, 1H), 6.87−6.84 (m, 1H), 6.82 (d, J = 8.4 Hz, 2H), 6.65 (d, J = 2.4 Hz, 1H), 2.79 (t, J = 6.4 Hz, 2H), 2.56−2.52 (m, 1H), 2.09−2.08 (m, 1H), 1.77−1.74 (m, 2H), 1.46−1.37 (m, 12H), 1.00−0.91 (m, 2H). ^{13}C NMR (100 MHz, DMSO-d_6) δ 181.39, 173.49, 161.76, 158.06, 156.86, 156.36, 156.21, 155.65, 130.67, 123.39, 121.21, 115.56, 109.18, 105.68, 101.74, 77.80, 46.35, 42.84, 37.68, 29.55, 28.73, 28.41 (Supporting Information Figs. S6 and S7). HRMS (ESI): calculated for $C_{28}H_{32}NO_8$, 510.2128 $[M+H]^+$; found 510.2114 (Supporting Information Fig. S8). Purity 98.3%.

The generation of reactive oxygen species is a contributor to aging-related skin damage and can occur from a minute fraction of oxygen being absorbed by the skin[51]. Antioxidants have been used to assist in preventing free radical-induced oxidative damage and promote skin health, and one example is α-lipoic acid (ALA). ALA is widely used as a food supplement and in skincare products[52]. ALA naturally exists in both *R* and *S* isomeric forms but encompasses poor bioavailability because of low absorption efficiency and tends to lose its properties in the presence of UV light due to its photosensitive structure[53–55]. Herein, we successfully obtained a conjugate of genistein with ALA, JW-191, 4-(5,7-dihydroxy-4-oxo-4*H*-chromen-3-yl)phenyl 5-(1,2-dithiolan-3-yl) pentanoate, following a similar synthetic method as mentioned above, to improve the photostability of ALA and retain ERβ

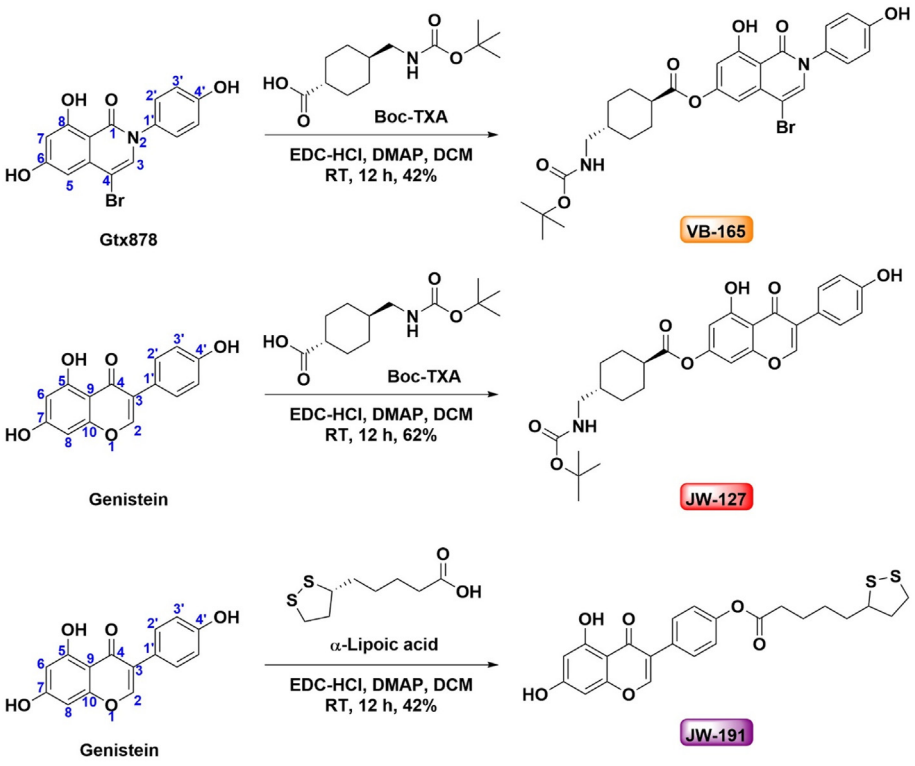

Scheme 1 Synthesis of ERβ agonist conjugates. Synthetic ERβ agonist GTx878 conjugated with tranexamic acid (TXA) to generate a monoester derivative, VB-165 (Top). Natural ERβ agonist genistein conjugated with TXA to yield a monoester derivative, JW-127 (Middle). Genistein conjugated with α-lipoic acid (ALA) to generate JW-191 (Bottom).

agonist activity (Scheme 1C), aiming to achieve additional benefits. Interestingly, the 4^1-OH group underwent esterification while 5- and 7-OH groups remained free as evidenced by the presence of signals at δ 12.84, 10.97 ppm respectively (Scheme 1C). ^{1}H NMR (400 MHz, DMSO-d_6) δ 12.84 (s, 1H), 10.97 (s, 1H), 8.45 (s, 1H), 7.59 (d, J = 8.8 Hz, 2H), 7.18 (d, J = 8.8Hz, 2H), 6.41 (d, J = 2.0 Hz, 1H), 6.23 (d, J = 2.0 Hz, 1H), 3.67−3.63 (m, 1H), 3.21−3.09 (m, 2H), 2.61 (t, J = 7.2 Hz, 2H), 2.46−2.38 (m, 1H), 1.93−1.84 (m, 1H), 1.73−1.55 (m, 4H), 1.50−1.44 (m, 2H). ^{13}C NMR (MHz, DMSO-d_6) δ 180.27, 172.20, 164.92, 162.42, 158.04, 155.52, 150.73, 130.57, 128.81, 122.14, 121.99, 104.87, 99.59, 94.28, 56.50, 38.59, 34.50, 33.75, 28.52, 24.55 (Supporting Information Figs. S9 and S10). HRMS (ESI): calculated for $C_{23}H_{23}O_6S_2$, 459.0936 $[M + H]^+$; found 459.0922 (Supporting Information Fig. S11). Purity 98.3%.

3.2. *In vitro validation of ERβ agonist conjugates' activity and selectivity*

Next, we employed an ER luciferase reporter assay using a 3x-ERE-TATA-*Luc* construct to validate the selectivity and potency of the synthesized compounds (Fig. 1A). In HEK-293 cells expressing ERα, none of our synthesized compounds, VB-165, JW-127, and JW-191, activated the ERα-responsive reporter, in contrast to the robust activation by a well-known ERα agonist, PPT (Fig. 1B). Instead, they all efficiently elicited ERβ activation just as the non-selective ER agonist ligand E2 did (Fig. 1C). When comparing activity in the presence of both ERs to only ERβ, VB-165 showed diminished activity, while JW-127 and JW-191 displayed overall enhanced activity (Fig. 1D). These changes could be related to the heterodimerization of ERα/β, implicating ligand selectivity of these compounds to ERβ existing as homodimers but also as ERα/β heterodimers[56]. Nonetheless, the synthesized conjugated compounds display potent activity that is selective to ERβ. Moreover, we performed dose−response experiments and found that JW-127 at 3 μmol/L significantly increases ERβ activation, at 2.5-fold greater activity than E2, and JW-191 at 10 μmol/L (Fig. 1E and F), suggesting modulation of agonist activity by the conjugated moieties.

3.3. *Administration of an ERβ agonist conjugate improves metabolic functions in aged mice*

Given the metabolic benefits of GTx878 in diet-induced obesity[27], we evaluated the effects of the GTx878 conjugate VB-165 on metabolic health in aging. Six-week treatment of VB-165 (Fig. 2A) caused a marginal decrease in body weight of 24-month-old mice (Fig. 2B), despite the slight increases in lean mass (Fig. 2C). This mild anti-obesity effect was underlined by a ~20% reduction in fat mass (Fig. 2D). In humans, dyslipidemia is an increased risk factor with aging[57]. Here we found plasma triglyceride levels to be reduced by approximately 40% after VB-165 administration (Fig. 2E). Insulin resistance is a representative hallmark of aging and the fundamental etiological factor of type 2 diabetes[58]. Notably, it was significantly improved by VB-165 treatment, as revealed by an insulin tolerance test (ITT) (Fig. 2F). We further assessed the blood composition of immune cells and detected a trending decrease in total white blood cells,

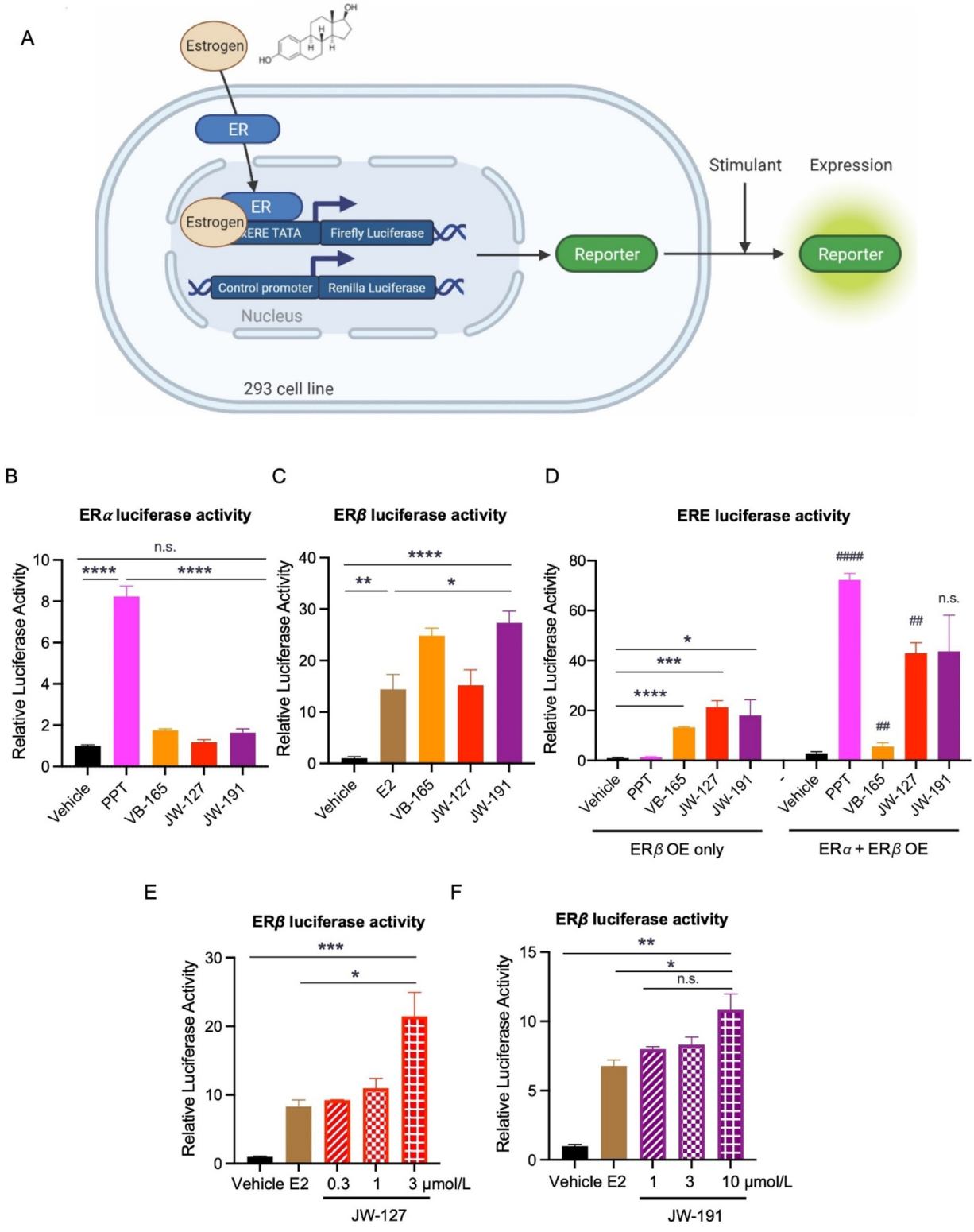

Figure 1 *In vitro* validation of the conjugates' selectivity and activity. (A) Dual luciferase ER reporter system in the HEK-293 cells. (B) ERα luciferase reporter activity. $n = 5$ (Vehicle, E2, VB-l65, JW-127); $n = 4$ (JW-191). All the compounds were at 1 mmol/L. (C−E) ERβ luciferase activity. (C) Comparing the ERβ activity of the conjugates. $n = 5$ (Vehicle, E2, VB-l65, JW-127), $n = 4$ (JW-191). (D) Assessing activity of the conjugates in the presence of both ERα and ERβ. $n = 4$ for all groups. The symbol "#" was denoted for statistical comparisons between the same treatment groups under the presence of either ERβ overexpression or both ERα and ERβ, $^{\#\#}P < 0.01$, $^{\#\#\#}P < 0.001$. (E) JW-127 dose response. $n = 3$ (Vehicle, E2: 1 mmol/L, JW-127: 0.3 mmol/L, JW-127: 1 mmol/L), $n = 5$ (JW-127: 3 mmol/L). (F) JW-191 dose response. $n = 3$ for all groups. E2, estradiol. PPT, subtype selective ERα agonist. $^{*}P < 0.05$, $^{**}P < 0.01$, $^{***}P < 0.001$, $^{****}P < 0.0001$, n.s., not significant. All values are presented as the mean ± SEM.

circulating lymphocytes, and neutrophils (Fig. 2G). Moreover, we observed a significant reduction in total monocyte numbers with treatment, implying protection against systemic inflammation, which is another hallmark of aging.

3.4. ERβ agonist conjugate treatment inhibits aging-associated visceral fat degeneration

As a vital organ for maintaining metabolic homeostasis, adipose tissue, particularly in the abdominal cavity, is a driver of aging[59]. Adipose tissue undergoes profound pathological remodeling in aging, such as hypertrophic expansion, inflammation, senescence, fibrosis, declined catabolism, and compromised adipogenesis[60]. The increase in adipocyte size, namely hypertrophy, is an indicator of compromised adipose function, correlating with all these pathological changes. Following the improvements in metabolic health observed in VB-165-treated mice, we proceeded to assess the state of their adipose tissue. The largest abdominal fat depot, epididymal white adipose tissue (eWAT), was reduced by over 60% in mass (Fig. 2H). This decrease in eWAT can be explained by a significantly smaller adipocyte size (Fig. 2I and J). Underpinning the inhibited adipocyte hypertrophy is the downregulation of the key lipogenic genes *Fasn* and *Scd1*, but not *Srebp1*, by VB-165 treatment (Fig. 2K). Interestingly, adipogenic programming was only modestly altered, with no changes in the expression of key adipocyte makers Perilipin and Adipsin, and only trending repression of the adipogenic transcription factor *Pparg2*. Moreover, there was a significant alleviation of adipose inflammation by VB-165 treatment, indicated by a lower detection of pan-macrophage marker F4/80 (Fig. 2L). Consistently, the inflammatory genes *Tnfa* and *Il6* were decreased (Fig. 2M). Together, activating ERβ shows potential in tackling pathological visceral adiposity that arises with aging. Of note is that visceral fat begins to expand in mid-age and is associated with a higher risk of eliciting metabolic complications than subcutaneous fat.

3.5. ERβ agonist conjugate treatment enhances catabolic function in subcutaneous adipose tissue

In contrast to eWAT, there was no change in inguinal subcutaneous white adipose tissue (sWAT) mass with VB-165 treatment (Fig. 3A). However, adipocyte size was similarly decreased as in eWAT (Fig. 3B and C), implying an increase in adipocyte numbers to compensate for size reduction in maintaining depot size. In support of this notion, the master adipogenic factor *Pparg2* was upregulated, while lipogenic genes *Scd1* and *Srebp1*, together with lipid droplet-coating gene *Perilipin*, were reduced (Fig. 3D). Fittingly, markers of adipose tissue brown remodeling that increase catabolic function, like *Ucp1, Elovl3*, and *Cidea*, were stimulated in the sWAT of treated mice (Fig. 3E). Taken together, the ERβ-selective agonist conjugate VB-165 shows coordinative effects on harnessing aging-associated degeneration in both eWAT and sWAT.

Further assessment of adipocyte biology under agonist treatment was carried out in differentiated 3T3-L1 adipocytes, a classic *in vitro* adipocyte model. Treatment of 3T3-L1 cells with VB-165 markedly attenuated neutral lipid accumulation during adipocyte development by Oil Red O and BODIPY staining, and this effect was reproduced by JW-127 (Fig. 3F). Supportively, these conjugates overall decreased the expression of genes involved in lipid storage, like *Perilipin*, *Srebp1*, *Scd1*, and *Fasn*, without suppressing the adipogenic gene, *Pparg2* (Fig. 3G). Interestingly, the white adipocyte marker *Adipsin* was downregulated, in contrast to the upregulated brown adipocyte marker *Ucp1*, channeling its *in vivo* catabolic properties. Moreover, we compared our agonist conjugates to their respective parent compounds, GTx-878, and genistein, and observed a largely similar trend in affecting adipocyte gene expression, though to different extents (Fig. 3G). The use of these compounds *in vitro* overall mimicked the effects observed *in vivo* in our aged mice, indicating that the direct effects of ERβ agonist conjugates on adipocytes contribute to their metabolic benefits with aging.

3.6. ERβ agonist conjugate treatment restrains aging-associated BAT whitening

Next, we extended our analyses to other important metabolic tissues to further evaluate the metabolic effects of the ERβ agonist conjugate VB-165. Brown adipose tissue (BAT) is a highly metabolically active organ imperative for non-shivering thermogenesis by consuming a large amount of lipids to dissipate energy as heat[61]. It gradually loses this ability and accumulates more lipids, morphing into WAT-like tissue, a process named "whitening" that occurs during aging[62]. Upon observing an induction of browning in sWAT and in adipocyte cultures, examination of BAT seemed fitting. Notably, compound treatment reverted this "whitening" morphology in the interscapular BAT (Fig. 4A). The protein levels of UCP1, which is the crucial protein for heat generation in BAT, significantly increased, while the lipid droplet-coating protein FABP4 was notably downregulated. Only modest decreases in white adipocyte-enriched adipokines Adiponectin (APN) and ADIPSIN were observed (Fig. 4B). Moreover, lipogenic genes *Srebf1* and *Scd1* were downregulated, together with white adipocyte marker *Adipsin* (Fig. 4C). These data together suggest restoration of BAT function in aging with ERβ agonist conjugate treatment.

3.7. ERβ agonist conjugates improve muscle function in aging

Both ERs are expressed in skeletal muscle, while ERβ has implications in muscle recovery, metabolism, and glucose uptake[10,63]. VB-165 treatment caused subtle changes in muscle histology (Fig. 5A). However, we detected an increase in *Pgc1a* expression, a key regulator of mitochondrial function in muscle (Fig. 5B). The glucose uptake gene *Glut4* was also mildly increased. Given these modest changes, we opted to assess this phenotype further in C2C12 cells, a common *in vitro* myoblast model. The use of agonists VB-165, JW-127, and JW-191 congruously enhanced the expression of *Pgc1a* and *Glut4*, phenocopying the *in vivo* effect (Fig. 5C). Interestingly, treatment with parent compounds showed similar trends, but were not as effective. ERβ agonist conjugate treatment also improved myogenesis, with increased expression of key myogenic markers *Acta1*, *MyoD*, and *MyoG* (Fig. 5D). The same trend was observed when parent compounds were used (Fig. 5D). Next, we examined whether the conjugates' effects were dependent on ERβ. To do this, we transfected pre-differentiated C2C12 myoblasts with a lentivirus containing sham shRNA (shSCR) or one targeting ERβ (shERβ), both expressing a GFP marker for validation (Fig. 5E). Expectingly, ERβ knockdown (encoded by *Esr2* gene) dampened the metabolic activity of C2C12 cells with the downregulation of genes *Glut4* and *Pgc1a* and blunted compound treatment (Fig. 5F). Differentiation was modestly compromised, with significant decreases in *Acta1* expression and

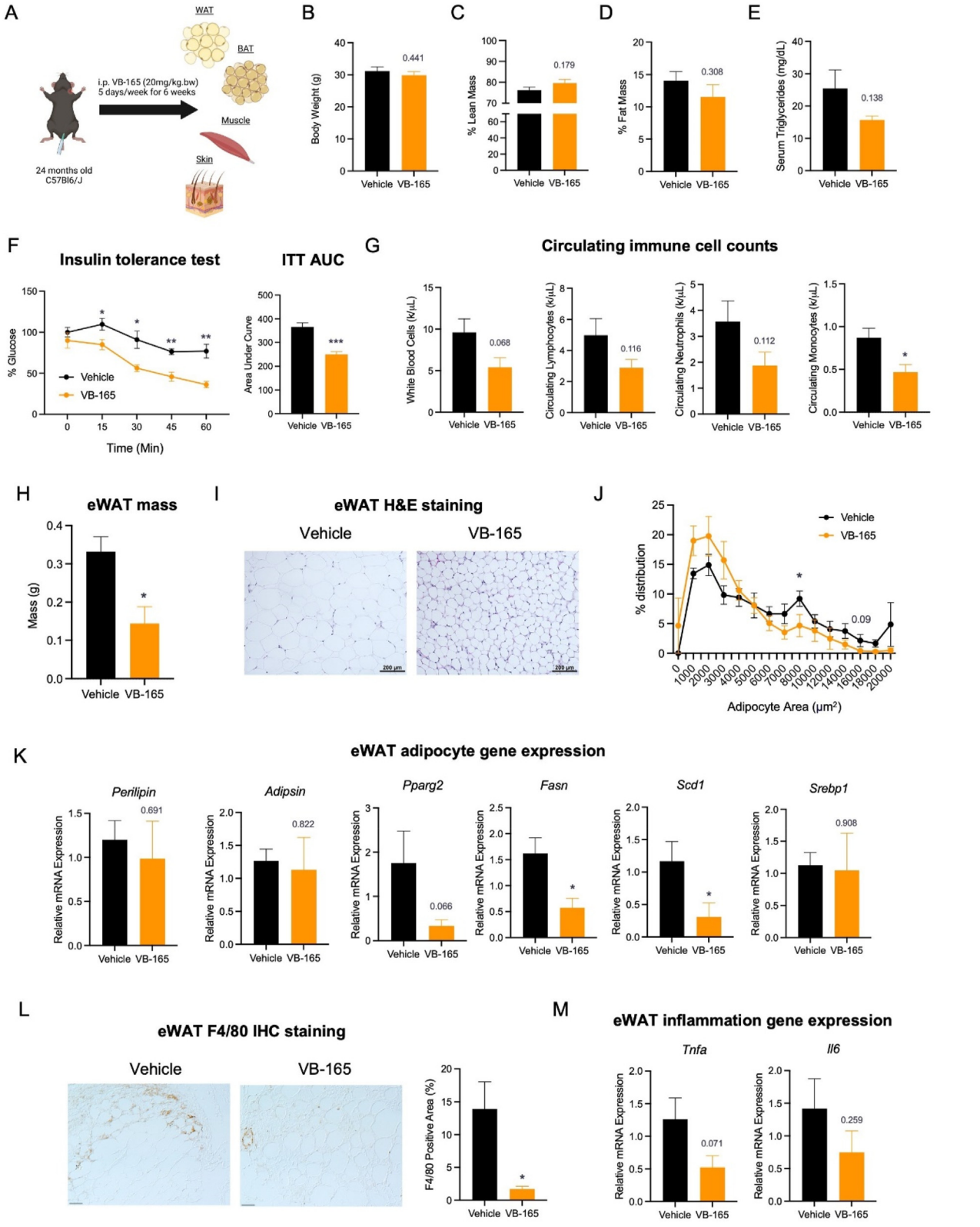

Figure 2 ERβ agonist conjugate VB-165 enhances metabolic health in aged mice. (A) Schematic of experimental study in 24-month-old mice receiving intraperitoneal injections of VB-165 for 6 weeks. Created with BioRender.com. (B) Body weight after the treatment. (C, D) Body composition after the treatment. (E) Serum triglyceride levels. (F) Intraperitoneal insulin tolerance tests (ITT) of aged mice with computed area under curve (AUC). (G) Profile of white blood cell counts. (H) Aged eWAT mass after compound treatment. (I) Hematoxylin and eosin (H&E) staining of eWAT. Scale bar, 200 μm. (J) Quantification of adipocyte size in eWAT. (K) Quantitative PCR (qPCR) analysis of adipogenic and lipogenic genes in eWAT. (L) Immunohistochemical (IHC) staining of pan-macrophage marker F4/80 in eWAT with quantification. Scale bar, 100 μm. (M) Inflammatory gene expression in eWAT. $^*P < 0.05$, $^{**}P < 0.01$, $^{***}P < 0.001$, $n = 5$. All values are presented as the mean ± SEM.

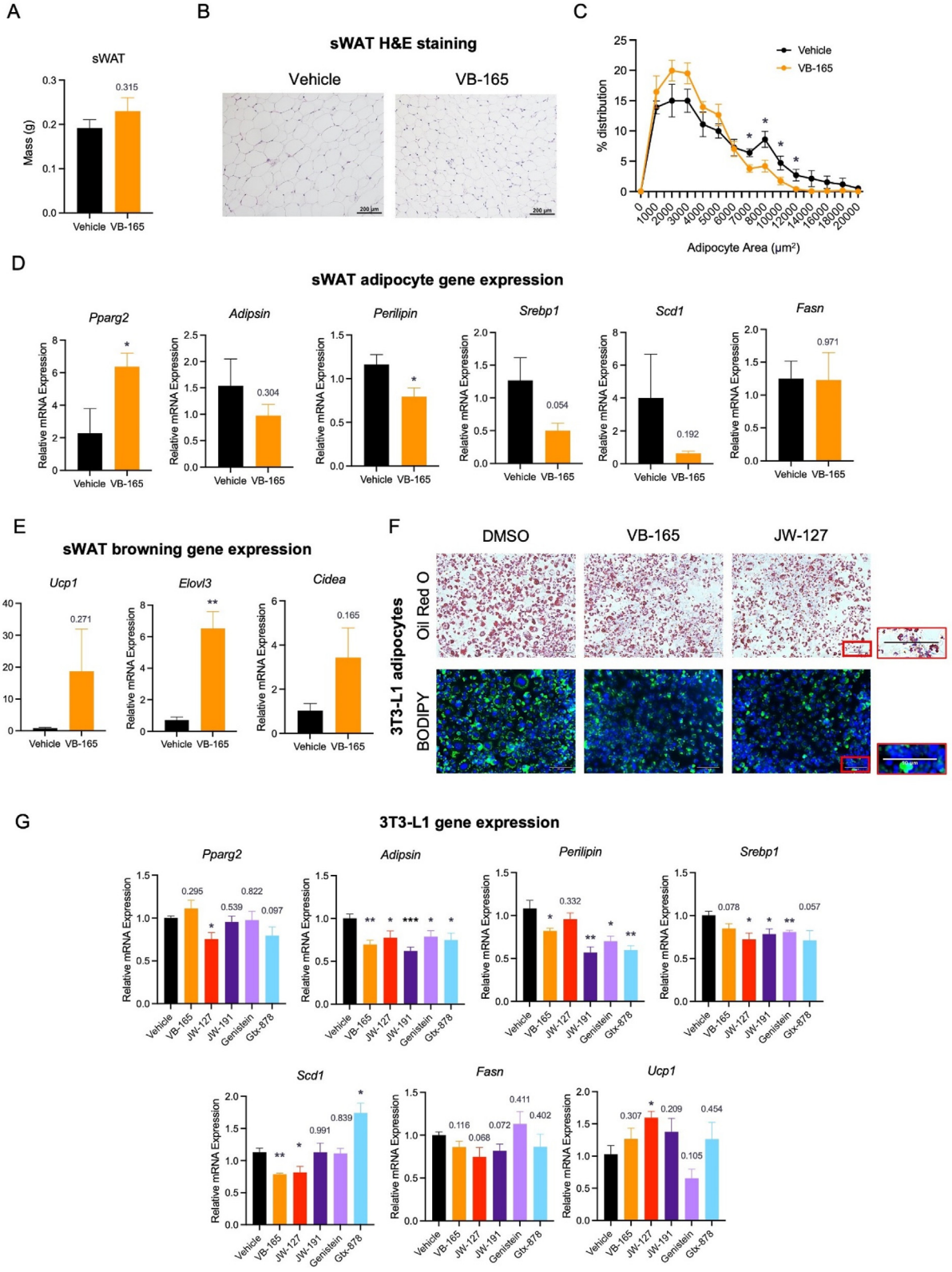

Figure 3 ERβ agonism improves adipose remodeling in subcutaneous fat. (A) Aged sWAT mass after the treatment. (B) H&E staining of sWAT. Scale bar, 200 μm. (C) Quantification of adipocyte size in sWAT. (D) qPCR analysis of adipogenic and lipogenic genes in sWAT; (E) The expression of brown adipocyte makers in sWAT. $*P < 0.05$, $**P < 0.01$, n.s., not significant, $n = 5$. (F) Oil Red O and BODIPY staining of 3T3-L1 adipocytes for neutral lipids. Scale bar, 50 μm. (G) qPCR analysis of adipogenic, lipogenic, and browning genes in differentiated 3T3-L1 adipocytes treated with agonist conjugates and parent compounds. $*P < 0.05$, $**P < 0.01$, $***P < 0.001$, $n = 4$ for all groups. All values are presented as the mean ± SEM.

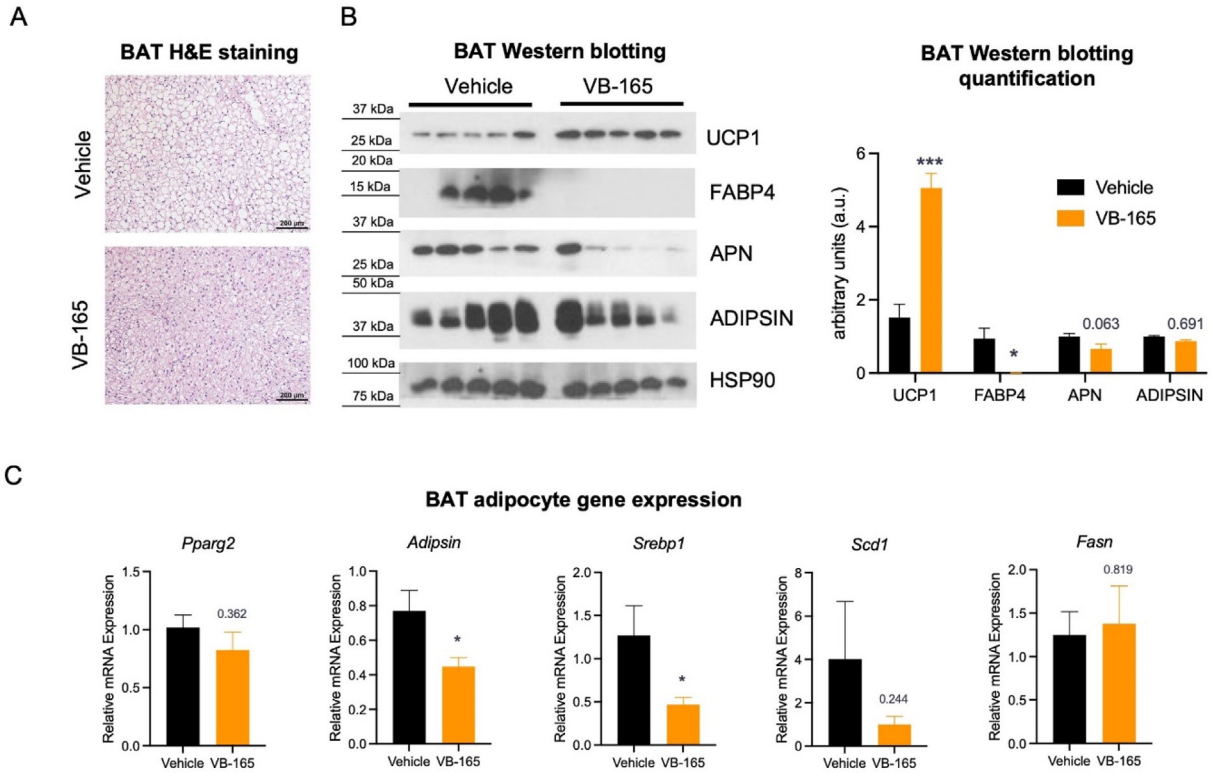

Figure 4 ERβ conjugate rejuvenates brown fat function in aging. (A) H&E staining of aged BAT after the treatment. (B) Western blotting of BAT proteins with quantifications. HSP90 was used as a loading control. (C) qPCR analysis of adipogenic and lipogenic genes in BAT. $*P < 0.05$, $***P < 0.001$, $n = 5$. All values are presented as the mean ± SEM.

subtle changes in *MyoD* and *MyoG* (Fig. 5D). Thus, we conclude that skeletal muscle is also a potential target tissue for selective ERβ agonists.

3.8. *ERβ agonist conjugates promote skin healing*

Aging is also associated with a decline in skin health, such as epidermis thinning and reduced skin cell proliferation[64]. ERβ is abundantly expressed in the skin. Given the broad anti-aging effects of our ERβ agonist VB-165 on metabolism, we assessed its implications on skin health. Whole-body treatment of VB-165 in aged mice promoted proliferation ($Ki67^+$) of skin basal cells ($p63^+$), as shown by a 2-fold increase in the number of proliferating basal cells ($p63^+Ki67^+$) (Fig. 6A and B). 6-Week treatment also increased epidermal thickness (Fig. 6C). Interestingly, we observed numerous $Ki67^+$ cells within the hair follicles (Fig. 6A), implicating a potential effect of the ERβ agonist conjugate on hair growth even with systemic delivery.

To further confirm the beneficial effects of ERβ activation on skin basal cell proliferation, we generated JW-191, which incorporates an anti-oxidative ALA conjugate of Genistein. Genistein has been shown to have several advantages in treating various skin pathologies[65–74]. Here, we employed an excision-induced skin injury model to study the immediate response of the conjugated drug[75]. Recovery was notably improved following treatment for 4 weeks, with a 3.5-fold increase in the numbers of proliferating basal cells in the epidermis (Fig. 6D and E). Moreover, the organization of the basal cell layer and underlying dermis was restored (Fig. 6F), in line with the beneficial effects observed in our experiments in aged mice treated with VB-165 (Fig. 6C).

To further demonstrate the connection between ERβ agonist conjugate treatment and skin health, we employed a frostbite-induced skin injury model where frozen magnets are placed on a shaved area of mice. ERβ agonist conjugates were then applied to the injured area for a period of one month (Fig. 7A). As a proof-of-concept, we chose two genistein conjugates, JW-127 and JW-191, which may provide additional benefits due to the conjugated TXA and ALA moieties, respectively (Fig. 7B and C). Notably, treatment with JW-127 and JW-191 improved wound healing, leading to a two-fold decrease in the injured area (Fig. 7B and C). Furthermore, conjugate treatment promoted skin healing with advanced coverage of epidermal cells in the injured area (Fig. 7D). We also observed a more than two-fold increase in the number of proliferating basal cells in the skin following treatments with both conjugates (Fig. 7E and F).

To elucidate whether ERβ regulates the proliferation of skin basal cells, we employed our previously mentioned lentivirus containing shRNA against ERβ to infect neonatal skin basal cells. ERβ knockdown led to modestly reduced transcript levels of *Esr2,* without affecting the expression of *Esr1*, the gene encoding ERα (Fig. 7G). Despite a slight decrease in the transcript levels of *Ki67*, a significant decrease in the proliferation of $Ki67^+$ basal cells was observed 4 days after knockdown (Fig. 7H and I). These findings confirm that our

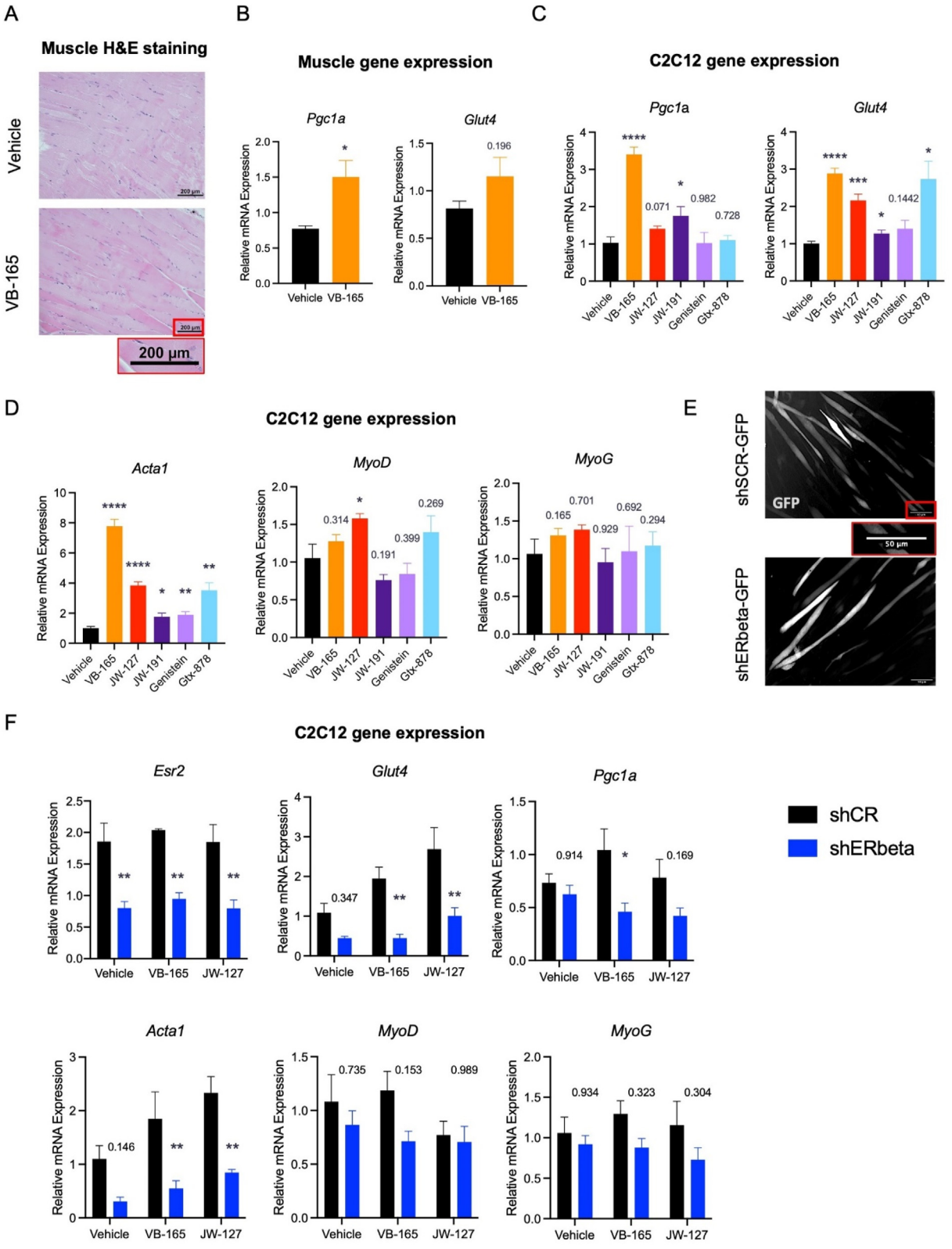

Figure 5 ERβ enhances skeletal muscle metabolism and integrity in aged mice. (A) H&E staining of aged skeletal muscle after the treatment. (B) Muscle gene expression. $^{*}P < 0.05$, n.s., not significant, $n = 5$. (C, D) Gene expression in C2C12 cells treated with agonist conjugates and parent compounds, $n = 4$ for all groups. (E) GFP-positive images of C2C12 cells infected with shRNA viruses to show infection efficiency (scramble or shERβ). Scale bar, 50 μm. (F) Gene expression in C2C12 cells after ERβ knockdown with agonist conjugate treatment. $^{*}P < 0.05$, $^{**}P < 0.01$, $^{***}P < 0.001$, $^{****}P < 0.0001$, $n = 4$ for all groups. All values are presented as the mean ± SEM.

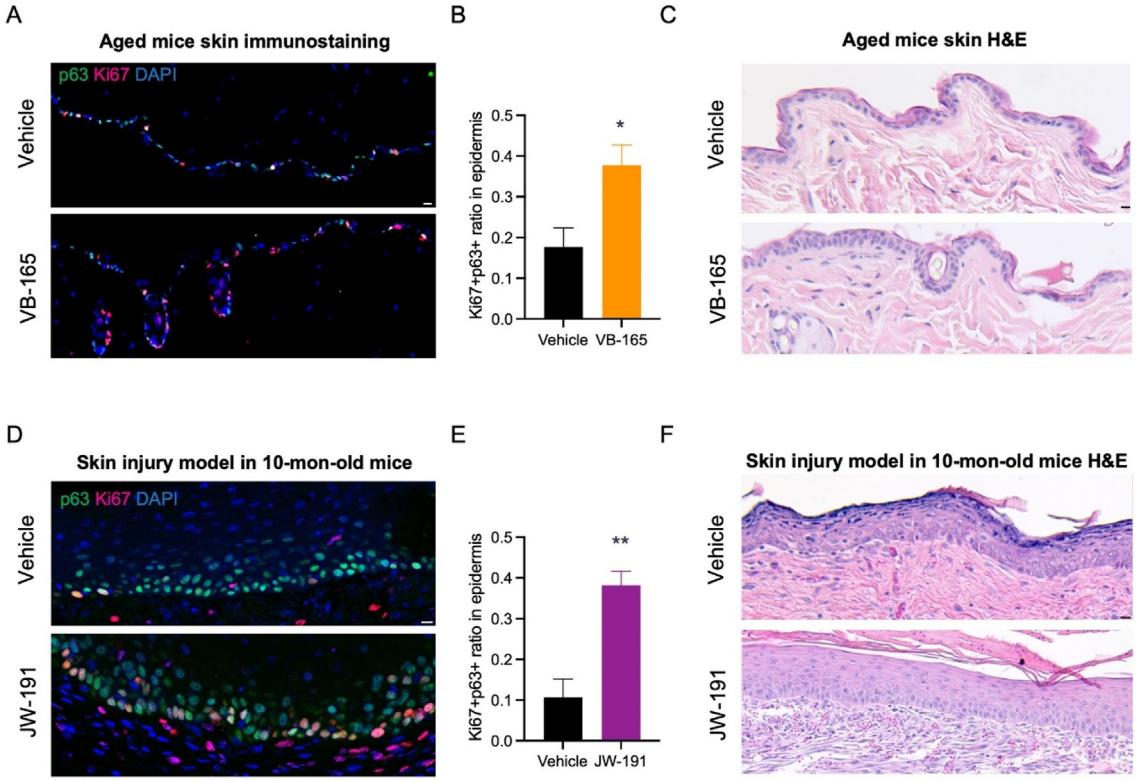

Figure 6 ERβ agonist conjugates enhance skin conditions. (A, B) Aged mouse skin slices were immunostained for Ki67 and p63 with quantification, under vehicle or VB-165 treatment. Scale bar, 10 μm. $*P < 0.05$, $n = 5$. (C) H&E staining of the skin in aged mice after VB-165 treatment. Scale bar, 10 μm. (D, E) Immunostaining of excision skin slices for Ki67 and p63, with quantification under vehicle or JW-191 treatment. Scale bars, 10 μm. $*P < 0.05$, $**P < 0.01$, $n = 4$. (F) H&E staining of excision skin between vehicle and JW-191 treatment groups. Scale bar, 10 μm. All values are presented as the mean ± SEM.

synthesized ERβ agonist conjugates improve the manifestations of skin health, including their proliferative ability, in addition to the benefits observed in aging-associated metabolic conditions.

4. Discussion

Specific ERβ ligands provide multiple beneficial effects in regards to aging and tissue regeneration. Here, we successfully synthesized conjugated compounds that activate ERβ with high specificity, confirming a multifaceted role for ERβ in cell integrity and health across several tissue types. These compounds are effective in improving insulin sensitivity and adipose remodeling in eWAT, sWAT, and BAT in aged mice. Moreover, treatment invoked positive metabolic changes in skeletal muscle worthy of further exploration. When gauging changes to the skin following drug application, we found an increase in the proliferation of basal progenitor cells in three models of skin injury: aging-, excision-, and frostbite-induced. Treatment with ERβ ligands attenuated skin injury accompanied by protected epidermal thickness.

All our three ERβ agonist conjugates, VB-165, JW-127, and JW-191, regardless of the synthetic or natural ligands used, have been shown beneficial in improving skin conditions. They can promote the proliferation of basal progenitor cells and accelerate the wound healing process. Conjugated TXA could provide additional benefits for remedying skin conditions. The antifibrinolytic molecule TXA was initially used in controlling heavy bleeding, especially during the menstrual cycle and nose bleeds[76–78]. It may have applications in wound healing by inhibiting fibrinolysis, a process responsible for the enzymatic breakdown of blood clots[79,80]. Another study reported that intradermal injection of TXA attenuates UV-induced expression of melanin in the melanocytes of guinea pigs. These findings support that TXA may be a suitable conjugate to ERβ agonists for achieving additive benefits[81].

Historically, the actions of estrogen and estradiol were attributed mostly to ERα[82]. However, the discovery of ERβ has reshaped the understanding of ER signaling and its relevance to metabolic health[83]. Studies in patients with polymorphisms of ERβ and in mice with genetic manipulations of ERβ display associations with body mass index, serum triglycerides, adiposity, as well as insulin signaling in many tissue types[26–31], even extending beyond adipose tissue. Several reports demonstrate a protective role for ERβ, whereas others suggest a possible pro-diabetogenic role[2,84–86]. Here we show a significant improvement in insulin resistance that is associated with aging when treated with ERβ-selective agonist conjugates.

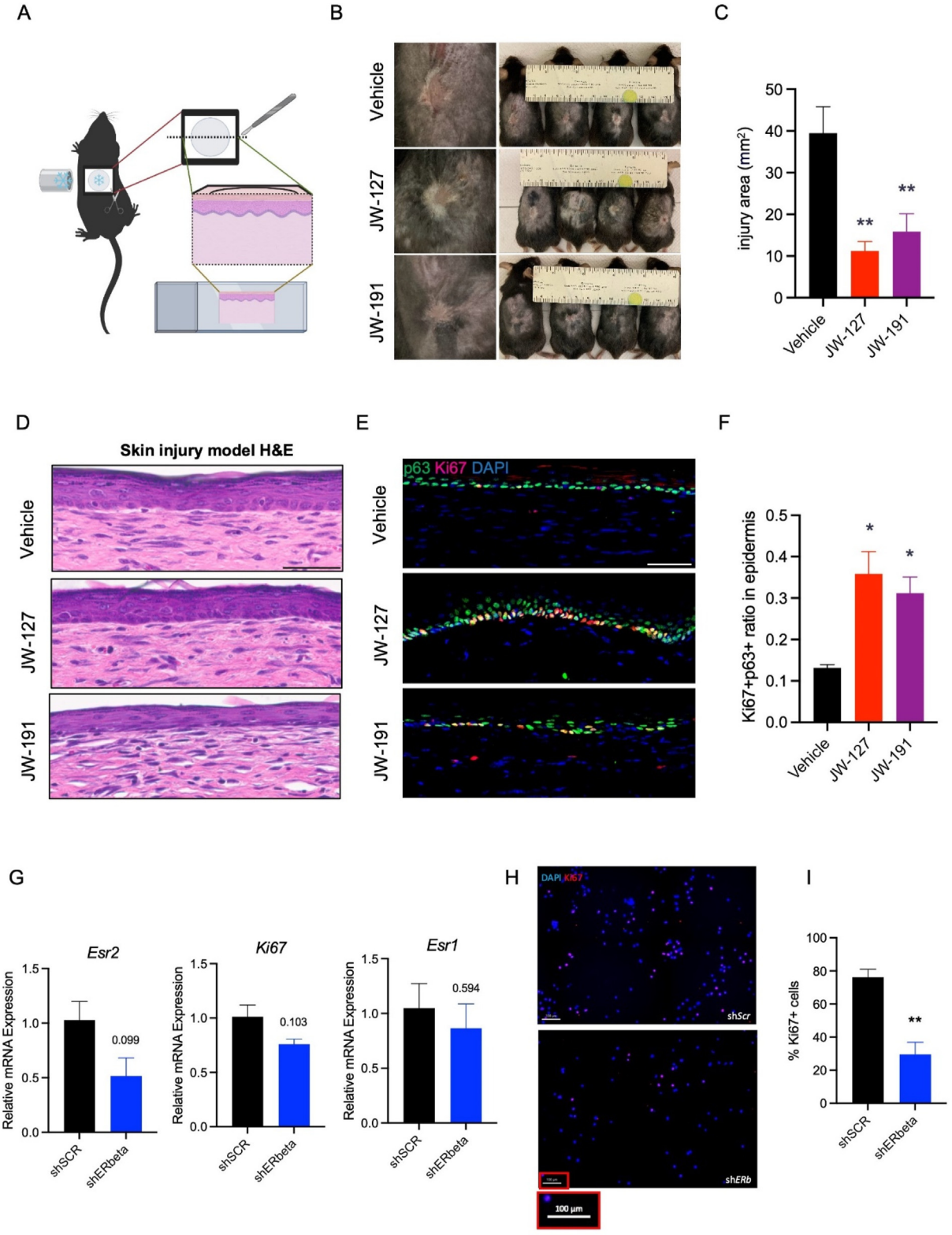

Figure 7 ERβ agonist conjugates promote skin injury healing. (A) Frostbite skin injury mouse model. (B, C) Skin closure 1 month after frostbite injury under treatment with vehicle, JW-127, or JW-191, and quantification. (D) H&E staining of skin recovered from frostbite injury under treatments. Scale bar, 50 µm. (E, F) Immunostaining of skin slices for Ki67 and p63, with quantification. Scale bar, 50 µm $*P < 0.05$. $**P < 0.01$, $n = 2, 4, 4$. (G) Gene expression in cultured basal skin cells after lentiviral ERβ knockdown using an shRNA. (H) Immunostaining of skin basal cells with Ki67 upon knockdown, with quantification (I). Scale bar, 100 µm $**P < 0.01$, $n = 3$. All values are presented as the mean ± SEM.

5. Conclusions

In the present study, we provide an alternative use of small molecule conjugates with agonist activity specific to ERβ. These compounds attenuated aging in mice through improving metabolic health, adipose functioning, and skeletal muscle integrity. Moreover, these compounds enhanced skin health by increasing wound recovery, epidermal thickness, and basal cell proliferation. Overall, the need for a highly selective yet sufficiently potent and consistent ERβ agonist warrants an investment in ER-based therapeutics. Our synthesized conjugates are distinct in their affinity, specificity, structure, and potency and, therefore, present as potential candidates in fulfilling these various needs.

Acknowledgments

This work was supported by the Columbia University startup packages (Li Qiang and Jianwen Que) and the University of Tennessee College of Pharmacy Drug Discovery Center (Wei Li).

Author contributions

Tarik Zahr: Investigation, Writing−Original Draft, Writing−Review & Editing, Visualization, Project administration, Formal analysis. Vijay K. Boda: Investigation, Writing−Original Draft, Project administration, Formal analysis. Jian Ge: Investigation, Project administration, Formal analysis. Lexiang Yu: Investigation. Zhongzhi Wu: Investigation. Jianwen Que: Conceptualization, Supervision, Methodology, Resources, Funding acquisition, Writing−Review & Editing. Wei Li: Conceptualization, Supervision, Methodology, Resources, Funding acquisition, Writing−Review & Editing. Li Qiang: Conceptualization, Supervision, Methodology, Resources, Funding acquisition, Writing−Review & Editing.

Conflicts of interest

A patent application is pending.

Appendix A. Supporting information

Supporting data to this article can be found online at https://doi.org/10.1016/j.apsb.2024.01.014.

References

1. Deroo BJ. Estrogen receptors and human disease. *J Clin Invest* 2006;**116**:561−70.
2. Barros RP, Gustafsson JÅ. Estrogen receptors and the metabolic network. *Cell Metabol* 2011;**14**:289−99.
3. Zhang Y, Howard BV, Cowan LD, Yeh J, Schaefer CF, Wild RA, et al. The effect of estrogen use on levels of glucose and insulin and the risk of type 2 diabetes in American Indian postmenopausal women. *Diabetes Care* 2002;**25**:500−4.
4. Yan H, Yang W, Zhou F, Li X, Pan Q, Shen Z, et al. Estrogen improves insulin sensitivity and suppresses gluconeogenesis *via* the transcription factor FoxO1. *Diabetes* 2019;**68**:291−304.
5. Bailey CJ, Ahmed-Sorour H. Role of ovarian hormones in the long-term control of glucose homeostasis. *Diabetologia* 1980;**19**:475−81.
6. Misso ML, Murata Y, Boon WC, Jones MEE, Britt KL, Simpson ER. Cellular and molecular characterization of the adipose phenotype of the aromatase-deficient mouse. *Endocrinology* 2003;**144**:1474−80.
7. Hevener AL, Clegg DJ, Mauvais-Jarvis F. Impaired estrogen receptor action in the pathogenesis of the metabolic syndrome. *Mol Cell Endocrinol* 2015;**418**:306−21.
8. Ko SH, Jung Y. Energy metabolism changes and dysregulated lipid metabolism in postmenopausal women. *Nutrients* 2021;**13**:4556.
9. Mauvais-Jarvis F, Clegg DJ, Hevener AL. The role of estrogens in control of energy balance and glucose homeostasis. *Endocr Rev* 2013;**34**:309−38.
10. Ikeda K, Horie-Inoue K, Inoue S. Functions of estrogen and estrogen receptor signaling on skeletal muscle. *J Steroid Biochem Mol Biol* 2019;**191**:105375.
11. Shah MG, Maibach HI. Estrogen and skin. *Am J Clin Dermatol* 2001;**2**:143−50.
12. Shu YY, Maibach HI. Estrogen and skin. *Am J Clin Dermatol* 2011;**12**:297−311.
13. Foryst-Ludwig A, Kintscher U. Metabolic impact of estrogen signalling through ERalpha and ERbeta. *J Steroid Biochem Mol Biol* 2010;**122**:74−81.
14. Jia M, Dahlman-Wright K, Gustafsson JÅ. Estrogen receptor alpha and beta in health and disease. *Best Pract Res Clin Endocrinol Metabol* 2015;**29**:557−68.
15. Liu Y, Ma H, Yao J. ERα, a key target for cancer therapy: a review. *OncoTargets Ther* 2020;**13**:2183−91.
16. Paterni I, Granchi C, Katzenellenbogen JA, Minutolo F. Estrogen receptors alpha (ERα) and beta (ERβ): subtype-selective ligands and clinical potential. *Steroids* 2014;**90**:13−29.
17. Shen K, Yu H, Xie B, Meng Q, Dong C, Shen K, et al. Anticancer or carcinogenic? The role of estrogen receptor β in breast cancer progression. *Pharmacol Ther* 2023;**242**:108350.
18. Božović A, Mandušić V, Todorović L, Krajnović M. Estrogen receptor beta: the promising biomarker and potential target in metastases. *Int J Mol Sci* 2021;**22**:1656.
19. McPherson SJ, Hussain S, Balanathan P, Hedwards SL, Niranjan B, Grant M, et al. Estrogen receptor-β activated apoptosis in benign hyperplasia and cancer of the prostate is androgen independent and TNFα mediated. *Proc Natl Acad Sci U S A* 2010;**107**:3123−8.
20. Rudolph A, Toth C, Hoffmeister M, Roth W, Herpel E, Jansen L, et al. Expression of oestrogen receptor β and prognosis of colorectal cancer. *Br J Cancer* 2012;**107**:831−9.
21. Xiao L, Xiao M, Zou M, Xu W. Estrogen receptor β inhibits prostate cancer cell proliferation through downregulating TGF-β1/IGF-1 signaling. *Int J Clin Exp Pathol* 2017;**10**:8569−76.
22. Heldring N, Pike A, Andersson S, Matthews J, Cheng G, Hartman J, et al. Estrogen receptors: how do they signal and what are their targets. *Physiol Rev* 2007;**87**:905−31.
23. Goulart AC, Zee RYL, Rexrode KM. Association of estrogen receptor 2 gene polymorphisms with obesity in women (obesity and estrogen receptor 2 gene). *Maturitas* 2009;**62**:179−83.
24. Koźniewski K, Wąsowski M, Jonas MI, Lisik W, Jonas M, Binda A, et al. Epigenetic regulation of estrogen receptor genes' expressions in adipose tissue in the course of obesity. *Int J Mol Sci* 2022;**23**:5989.
25. Ponnusamy S, Tran QT, Harvey I, Smallwood HS, Thiyagarajan T, Banerjee S, et al. Pharmacologic activation of estrogen receptor α increases mitochondrial function, energy expenditure, and brown adipose tissue. *FASEB J* 2017;**31**:266−81.
26. González-Granillo M, Savva C, Li X, Fitch M, Pedrelli M, Hellerstein M, et al. ERβ activation in obesity improves whole body metabolism *via* adipose tissue function and enhanced mitochondria biogenesis. *Mol Cell Endocrinol* 2019;**479**:147−58.
27. Yepuru M, Eswaraka J, Kearbey JD, Barrett CM, Raghow S, Veverka KA, et al. Estrogen receptor-β-selective ligands alleviate high-fat diet- and ovariectomy-induced obesity in mice. *J Biol Chem* 2010;**285**:31292−303.
28. Weigt C, Hertrampf T, Kluxen FM, Flenker U, Hülsemann F, Fritzemeier KH, et al. Molecular effects of ER alpha- and beta-selective agonists on regulation of energy homeostasis in obese female Wistar rats. *Mol Cell Endocrinol* 2013;**377**:147−58.

29. Velders M, Schleipen B, Fritzemeier KH, Zierau O, Diel P. Selective estrogen receptor-β activation stimulates skeletal muscle growth and regeneration. *FASEB J* 2012;**26**:1909−20.
30. Seko D, Fujita R, Kitajima Y, Nakamura K, Imai Y, Ono Y. Estrogen receptor β controls muscle growth and regeneration in young female mice. *Stem Cell Rep* 2020;**15**:577−86.
31. Parr MK, Zhao P, Haupt O, Ngueu ST, Hengevoss J, Fritzemeier KH, et al. Estrogen receptor beta is involved in skeletal muscle hypertrophy induced by the phytoecdysteroid ecdysterone. *Mol Nutr Food Res* 2014;**58**:1861−72.
32. Inoue T, Miki Y, Abe K, Hatori M, Hosaka M, Kariya Y, et al. The role of estrogen-metabolizing enzymes and estrogen receptors in human epidermis. *Mol Cell Endocrinol* 2011;**344**:35−40.
33. Thornton Mj, Taylor AH, Mulligan K, Al-Azzawi F, Lyon CC, O'Driscoll J, et al. The distribution of estrogen receptor β is distinct to that of estrogen receptor α and the androgen receptor in human skin and the pilosebaceous unit. *J Invest Dermatol Symp Proc* 2003;**8**:100−3.
34. Krahn-Bertil E, Dos Santos M, Damour O, Andre V, Bolzinger MA. Expression of estrogen-related receptor beta (ERRβ) in human skin. *Eur J Dermatol* 2010;**20**:719−23.
35. Csekes E, Račková L. Skin aging, cellular senescence and natural polyphenols. *Int J Mol Sci* 2021;**22**:12641.
36. Chang KC, Wang Y, Oh IG, Jenkins S, Freedman LP, Thompson CC, et al. Estrogen receptor β is a novel therapeutic target for photoaging. *Mol Pharmacol* 2010;**77**:744−50.
37. Vitale DC, Piazza C, Melilli B, Drago F, Salomone S. Isoflavones: estrogenic activity, biological effect and bioavailability. *Eur J Drug Metab Pharmacokinet* 2013;**38**:15−25.
38. Kitagawa S, Inoue K, Teraoka R, Morita S. Enhanced skin delivery of genistein and other two isoflavones by microemulsion and prevention against UV irradiation-induced erythema formation. *Chem Pharm Bull* 2010;**58**:398−401.
39. Vu QL, Fang CW, Suhail M, Wu PC. Enhancement of the topical bioavailability and skin whitening effect of genistein by using microemulsions as drug delivery carriers. *Pharmaceuticals* 2021;**14**:1233.
40. Tian L, Yang Y, Wysocki LM, Arnold AC, Hu A, Ravichandran B, et al. Selective esterase−ester pair for targeting small molecules with cellular specificity. *Proc Natl Acad Sci U S A* 2012;**109**:4756−61.
41. Huang HT, Brand OM, Mathew M, Ignatiou C, Ewen EP, Mccalmon SA, et al. Myomaxin is a novel transcriptional target of MEF2A that encodes a Xin-related α-actinin-interacting protein. *J Biol Chem* 2006;**281**:39370−9.
42. Dill TL, Carroll A, Pinheiro A, Gao J, Naya FJ. The long noncoding RNA Meg3 regulates myoblast plasticity and muscle regeneration through epithelial-mesenchymal transition. *Development* 2020;**148**:dev194027.
43. Wan Q, Calhoun C, Zahr T, Qiang L. Uncoupling lipid synthesis from adipocyte development. *Biomedicines* 2023;**11**:1132.
44. He Y, B'nai Taub A, Yu L, Yao Y, Zhang R, Zahr T, et al. PPARγ acetylation orchestrates adipose plasticity and metabolic rhythms. *Adv Sci* 2023;**10**:2204190.
45. Pedram A, Razandi M, Korach KS, Narayanan R, Dalton JT, Levin ER. ERβ selective agonist inhibits angiotensin-induced cardiovascular pathology in female mice. *Endocrinology* 2013;**154**:4352−64.
46. Yepuru M, Wu Z, Kulkarni A, Yin F, Barrett CM, Kim J, et al. Steroidogenic enzyme AKR1C3 is a novel androgen receptor-selective coactivator that promotes prostate cancer growth. *Clin Cancer Res* 2013;**19**:5613−25.
47. Narayanan R, Ahn S, Cheney MD, Yepuru M, Miller DD, Steiner MS, et al. Selective androgen receptor modulators (SARMs) negatively regulate triple-negative breast cancer growth and epithelial:mesenchymal stem cell signaling. *PLoS One* 2014;**9**:e103202.
48. Narayanan R, Yepuru M, Szafran AT, Szwarc M, Bohl CE, Young NL, et al. Discovery and mechanistic characterization of a novel selective nuclear androgen receptor exporter for the treatment of prostate cancer. *Cancer Res* 2010;**70**:842−51.
49. Lee JH, Park JG, Lim SH, Kim JY, Ahn KY, Kim MY, et al. Localized intradermal microinjection of tranexamic acid for treatment of melasma in Asian patients: a preliminary clinical trial. *Dermatol Surg* 2006;**32**:626−31.
50. Muthyala RS, Ju YH, Sheng S, Williams LD, Doerge DR, Katzenellenbogen BS, et al. Equol, a natural estrogenic metabolite from soy isoflavones. *Bioorg Med Chem* 2004;**12**:1559−67.
51. Poljšak B, Dahmane RG, Godić A. Intrinsic skin aging: the role of oxidative stress. *Acta Dermatovenerol Alpina* 2012;**21**:33−6.
52. Ruey JY, Vanscott EJ, assignee. *N*-Lipoic-amino acid or peptide, derivatives and their uses. 2021 October 26. United States patent US11155531B2.
53. Wada N, Wakami H, Konishi T, Matsugo S. The degradation and regeneration of α-lipoic acid under the irradiation of UV light in the existence of homocysteine. *J Clin Biochem Nutr* 2009;**44**:218−22.
54. Matsugo S, Bito T, Konishi T. Photochemical stability of lipoic acid and its impact on skin ageing. *Free Radic Res* 2011;**45**:918−24.
55. Kofuji K, Isobe T, Murata Y. Controlled release of alpha-lipoic acid through incorporation into natural polysaccharide-based gel beads. *Food Chem* 2009;**115**:483−7.
56. Coriano CG, Liu F, Sievers CK, Liang M, Wang Y, Lim Y, et al. A computational-based approach to identify estrogen receptor α/β heterodimer selective ligands. *Mol Pharmacol* 2018;**93**:197−207.
57. Liu HH, Li JJ. Aging and dyslipidemia: a review of potential mechanisms. *Ageing Res Rev* 2015;**19**:43−52.
58. Carrascosa MJ, Andres A, Ros M, Bogonez E, Arribas C, Fernandez-Agullo T, et al. Development of insulin resistance during aging: involvement of central processes and role of adipokines. *Curr Protein Pept Sci* 2011;**12**:305−15.
59. Tchkonia T, Morbeck DE, Von Zglinicki T, Van Deursen J, Lustgarten J, Scrable H, et al. Fat tissue, aging, and cellular senescence. *Aging Cell* 2010;**9**:667−84.
60. Ou MY, Zhang H, Tan PC, Zhou SB, Li QF. Adipose tissue aging: mechanisms and therapeutic implications. *Cell Death Dis* 2022;**13**:300.
61. Zhang Z, Yang D, Xiang J, Zhou J, Cao H, Che Q, et al. Non-shivering thermogenesis signalling regulation and potential therapeutic applications of brown adipose tissue. *Int J Biol Sci* 2021;**17**:2853−70.
62. Schosserer M, Grillari J, Wolfrum C, Scheideler M. Age-induced changes in white, brite, and brown adipose depots: a mini-review. *Gerontology* 2018;**64**:229−36.
63. Rüegg J, Cai W, Karimi M, Kiss NB, Swedenborg E, Larsson C, et al. Epigenetic regulation of glucose transporter 4 by estrogen receptor β. *Mol Endocrinol* 2011;**25**:2017−28.
64. Zou Z, Long X, Zhao Q, Zheng Y, Song M, Ma S, et al. A single-cell transcriptomic atlas of human skin aging. *Dev Cell* 2021;**56**:383−97.
65. Barnes S. Evolution of the health benefits of soy isoflavones. *Exp Biol Med* 1998;**217**:386−96.
66. Anderson JJB, Ambrose WW, Garner SC. Biphasic effects of genistein on bone tissue in the ovariectomized, lactating rat model. *Exp Biol Med* 1998;**217**:345−50.
67. Honoré EK, Koudy Williams J, Anthony MS, Clarkson TB. Soy isoflavones enhance coronary vascular reactivity in atherosclerotic female macaques. *Fertil Steril* 1997;**67**:148−54.
68. Potter SM, Baum JA, Teng H, Stillman RJ, Shay NF, Erdman JW. Soy protein and isoflavones: their effects on blood lipids and bone density in postmenopausal women. *Am J Clin Nutr* 1998;**68**:1375S. 79S.
69. Čoma M, Lachová V, Mitrengová P, Gál P. Molecular changes underlying genistein treatment of wound healing: a review. *Curr Issues Mol Biol* 2021;**43**:127−41.
70. Marini H, Polito F, Altavilla D, Irrera N, Minutoli L, Calò M, et al. Genistein aglycone improves skin repair in an incisional model of wound healing: a comparison with raloxifene and oestradiol in ovariectomized rats. *Br J Pharmacol* 2010;**160**:1185−94.
71. Tie L, An Y, Han J, Xiao Y, Xiaokaiti Y, Fan S, et al. Genistein accelerates refractory wound healing by suppressing superoxide and FoxO1/iNOS pathway in type 1 diabetes. *J Nutr Biochem* 2013;**24**:88−96.

72. Emmerson E, Campbell L, Ashcroft GS, Hardman MJ. The phytoestrogen genistein promotes wound healing by multiple independent mechanisms. *Mol Cell Endocrinol* 2010;**321**:184−93.
73. Eo H, Lee HJ, Lim Y. Ameliorative effect of dietary genistein on diabetes induced hyper-inflammation and oxidative stress during early stage of wound healing in alloxan induced diabetic mice. *Biochem Biophys Res Commun* 2016;**478**:1021−7.
74. Park E, Lee SM, Jung IK, Lim Y, Kim JH. Effects of genistein on early-stage cutaneous wound healing. *Biochem Biophys Res Commun* 2011;**410**:514−9.
75. Wang X, Ge J, Tredget EE, Wu Y. The mouse excisional wound splinting model, including applications for stem cell transplantation. *Nat Protoc* 2013;**8**:302−9.
76. Hurskainen R, Leminen. Tranexamic acid for the treatment of heavy menstrual bleeding: efficacy and safety. *Int J Womens Health* 2012;**4**:413−21.
77. Ker K, Edwards P, Perel P, Shakur H, Roberts I. Effect of tranexamic acid on surgical bleeding: systematic review and cumulative meta-analysis. *BMJ* 2012;**344**:e3054.
78. Lukes AS, Moore KA, Muse KN, Gersten JK, Hecht BR, Edlund M, et al. Tranexamic acid treatment for heavy menstrual bleeding. *Obstet Gynecol* 2010;**116**:865−75.
79. Jonathan D, Tamar G, Nyoman G, Mario I, Hussein K, Edward K, et al. The importance of early treatment with tranexamic acid in bleeding trauma patients: an exploratory analysis of the CRASH-2 randomised controlled trial. *Lancet* 2011;**377**:1096−101.
80. Cesarman-Maus G, Hajjar KA. Molecular mechanisms of fibrinolysis. *Br J Haematol* 2005;**129**:307−21.
81. Li D, Shi Y, Li M, Liu J, Feng X. Tranexamic acid can treat ultraviolet radiation-induced pigmentation in Guinea pigs. *Eur J Dermatol* 2010;**20**:289−92.
82. Tang ZR, Zhang R, Lian ZX, Deng SL, Yu K. Estrogen-receptor expression and function in female reproductive disease. *Cells* 2019;**8**:1123.
83. Kuiper GG, Enmark E, Pelto-Huikko M, Nilsson S, Gustafsson JA. Cloning of a novel receptor expressed in rat prostate and ovary. *Proc Natl Acad Sci U S A* 1996;**93**:5925−30.
84. Davezac M, Buscato M, Zahreddine R, Lacolley P, Henrion D, Lenfant F, et al. Estrogen receptor and vascular aging. *Front Aging* 2021;**2**:727380.
85. Foryst-Ludwig A, Clemenz M, Hohmann S, Hartge M, Sprang C, Frost N, et al. Metabolic actions of estrogen receptor beta (ERβ) are mediated by a negative cross-talk with PPARγ. *PLoS Genet* 2008;**4**:e1000108.
86. Kamble PG, Pereira MJ, Almby K, Eriksson JW. Estrogen interacts with glucocorticoids in the regulation of lipocalin 2 expression in human adipose tissue. Reciprocal roles of estrogen receptor α and β in insulin resistance?. *Mol Cell Endocrinol* 2019;**490**:28−36.